

Lasers in Manufacturing Conference 2021

Direct laser writing of metal nanostructures from the gas phase by two-photon-absorption process

Nicolai Schwarz^{a, b, *}, Michael Bassler^a, Thomas Walther^b, Thomas Klotzbuecher^a

^aFraunhofer Institut für Mikrotechnik und Mikrosysteme, Carl-Zeiss-Strasse 18-20, 55129 Mainz, Germany

^bInstitut für Angewandte Physik, Schlossgartenstrasse 7, 64289 Darmstadt, Germany

Abstract

A new approach for the generation of three-dimensional metal nanostructures, based on two-photon-absorption (TPA) of fs-laser radiation on silver-precursor molecules in the gas phase, is introduced. For that, a mode-locked fs-laser of 800 nm central wavelength and a pulse duration of 10 fs at a frequency of 76 MHz is used. The deposition process is performed in a vacuum chamber, allowing for evaporating a liquid organometallic silver-precursor under controlled temperature and pressure conditions. An inverse microscope objective of NA=0.65 and a working distance of 0.57 mm is used to focus the beam through a sapphire window onto a substrate, fixed in the vacuum chamber. The focus is moved in space by means of a piezo-driven stage with nm-resolution. Two-dimensional silver structures with dimensions in the sub-micrometer range are successfully deposited from the gas phase on glass substrates. Future investigations aim for extending the method into the third dimension.

Keywords: two-photon absorption; femtosecond laser direct writing; metallic nanostructures; gas-phase; silver precursor

1. Introduction

The fabrication of metallic 3D-nanostructures recently received a lot of attention via new applications in plasmonics, like e.g. metamaterials with a negative refractive index for optical cloaking or non-diffraction-limited optics (Zi Jing Wong et al., 2017). Furthermore, metallic nanostructures find application in surface enhanced Raman scattering (Seniutinas et al., 2015), catalytic reactions (Zarzar et al., 2012), optical sensing (Yokota et al., 2009) and electronic interconnection with metal nanowires (Xu et al., 2010).

* Corresponding author.

E-mail address: nicolai.schwarz@imm.fraunhofer.de.

There exist various methods (Hirt et al., 2017) for generating metallic nanostructures, among which focused electron beam induced deposition (FEBID) is one of the most promising. FEBID deposits metallic nanostructures below the diffraction limit from the gas phase. However, pressures in the range of high vacuum as well as elaborate equipment for the delivery of the electron beam are required. A very good overview of other methods used for direct writing of metallic nanostructures and the progress made in this field during the last years, is given in the paper of Hirt et al., 2017.

In the present paper, we introduce a new method based on two-photon-absorption (TPA) of fs-laser radiation on silver-containing molecules in the gas phase, thereby leading to a smaller interaction zone, compared to a single-photon absorption (SPA) process. Laser direct writing of metallic structures via SPA out of the gas phase, has already been successfully demonstrated by Stuke et al., 1991. However, the minimal, diffraction limited structure size that can be achieved by SPA lies in the range of several microns. With the two-photon-absorption deposition process, which is well known from the laser direct writing of nanostructures in SU-8 or ormocer resists, much smaller structure sizes can be attained, due to intensity constraints in the focus zone. The nanostructures produced in this way can be metallized in a subsequent step by means of electroplating (e.g. with silver), but the problem with this technique is that a selective metallization of the nanostructures is not possible and thus the functionality of metallic nanostructures is only given, if detached from the substrate, which is difficult to achieve (Radke et al., 2011). Another method to produce metallic nanostructures by LDW techniques using TPA is the reduction of silver nitrate in an aqueous solution (Ishikawa et al., 2012). However, when separating the nanostructures from the liquid phase, the substrate must always be wetted, which is time-consuming and involves additional cleaning steps, particularly when deposition is made on pre-structured functional substrates (e.g. wafers). By combining the TPA with LDW from the gas phase, we want to overcome these obstacles.

2. Experimental Setup, Materials and Methods

2.1. Experimental Setup

A femtosecond Ti:Sapphire laser femto-scientific pro from Femtolasers with a central wavelength of 800 nm and a pulse duration of about 10 fs is used for the TPA-based deposition. Figure 1 provides a schematic overview of the optical setup.

The laser beam dose on the substrate is controlled via a shutter which has an aperture of 1 mm, a very short delay time of 0.54 ms and a minimum exposure time of 0.93 ms. A continuous gray filter wheel (OD 0.04 to 3.0) is used for variable beam attenuation. The beam is expanded by a beam expansion unit, consisting of a microscope objective Obj1 (20x, NA 0.4, $f = 5.85$ mm) and a collimator lens L1 ($f = 20$ mm), to a diameter of 6 mm.

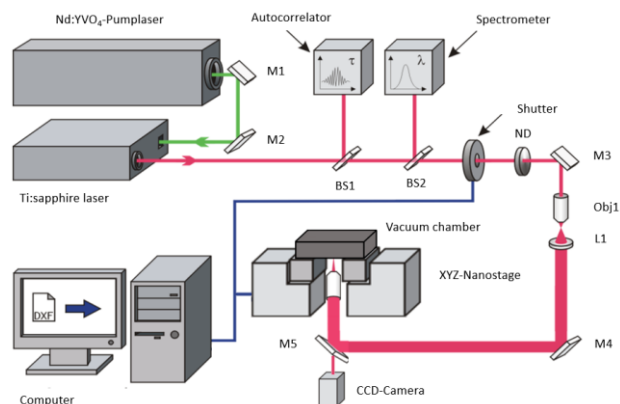


Fig. 1. Scheme of the optical setup for direct laser writing of structures using TPA. M = mirror, L = lens, BS = beam splitter, ND = gray filter, Obj = microscope objective

The beam is coupled into the vacuum chamber via the mirrors M4, and the beam splitter M5 and an inverse microscope objective (40x, NA 0.65). Due to the expansion of the beam, the wings of the gaussian beam intensity profile are cut off at the aperture of the objective, delivering a more homogeneous illumination of the microscope objective and thus leading to an improved aspect ratio of the beam waist. The focal position of the beam is set onto the glass substrate surface along the z-axis, using a piezoelectric positioning unit, moving the inverse objective. The focal plane is controlled by means of a CCD camera attached behind the beam splitter M5.

The liquid precursor is evaporated in a specially designed reaction chamber. The reaction chamber has an inlet for nitrogen purge gas, an outlet to the vacuum pump and a reservoir containing the precursor. After evacuation of the chamber, it was heated to temperatures of 303 K to 323 K. The concentration of the gaseous precursor is measured indirectly with the help of the partial pressure, recorded by a capacitive pressure sensor, mounted at the chamber. The vapor pressure typically is in the mbar range and is adjusted by means of the vapor pressure curve of the organometallic precursor. The fs-laser beam is coupled into the chamber through a sapphire glass window and focused onto the substrate surface.

Preliminary experiments with SPA were executed with a cw diode laser having a power of 150 mW and a wavelength of 405 nm. The laser was focused on a glass substrate with a thin film of liquid precursor on its surface. Further experiments were executed with an OPTEC Micromaster excimer laser with a wavelength of 193 nm, pulse duration of 18 ns and pulse repetition rate of 300 Hz. Experiments were carried out in a vacuum chamber containing a reservoir for evaporation of the precursor. A quartz substrate was installed at a small distance above the reservoir to get a high concentration of gaseous precursor molecules.

2.2. Materials

For the experiments the organometallic precursor (hfac)Ag(VTES), from abcr GmbH was used. The two ligands binding to the silver atom are hexafluoroacetylacetone (hfac) and vinyltriethylsilane (VTES). The choice of different ligands affect properties like photon absorption, evaporation temperature and state of matter of the resulting precursor complex. (hfac)Ag(VTES) shows a number of properties that are well suited for the process. It is easy to handle, to store and can be applied directly in the process chamber, since the

precursor is liquid at room temperature. Gaseous precursors on the contrary are more difficult to handle and solid precursors often exhibit high evaporation temperatures. Furthermore, the comparatively low evaporation temperature of 303-323 K can be easily and precisely set with ordinary heating equipment (Barth et al., 2020). In order to meet the goal of higher spatial resolution through TPA, it is important that the precursor does not show significant absorption around 800 nm, the operating wavelength of the fs-laser, thus preventing SPA. Therefore, the ideal absorption maximum should be around 400 nm. The absorption peak of (hfac)Ag(VTES) lies in the range of 280-350 nm, as determined by UV-VIS spectroscopy, so that SPA processes can be ruled out.

As substrates glass sheets of thickness 1 mm have been used that have been cut to a size of 5x5 mm². Some experiments were executed on indium tin oxide (ITO) substrates of identical size to circumvent the disadvantage of substrate charging during SEM measurements.

2.3. Structural Analysis

The deposited structures were examined by scanning electron microscope (SEM), using a LEO 1550 VP to determine the morphology of the material. In addition, energy dispersive X-ray spectroscopy (EDX) with an Oxford INCA II was made. Optical (Leica DM8000) as well as white light interferometry microscopes (Bruker ContourGT-K) were used, to evaluate the height and width of the structures. In case of glass substrates it was necessary to sputter the surfaces of the glass substrate after deposition of silver structures with a 30 nm gold layer, to prevent the surface from electrical charging during SEM and to obtain reflective surfaces, required for white light interferometry.

3. Experimental Results

Firstly it was investigated, whether the (hfac)Ag(VTES) precursor is suitable for SPA. For that, a mixture of 0.05 molar of toluene and (hfac)Ag(VTES) was exposed to a 405 nm diode laser. The precursor's concentration was set to a value comparable to that used in the gas phase during TPA. As a result, small islands of granular silver, whose size correlates with the exposure time, were achieved, demonstrating that SPA-based decomposition of the precursor in the liquid phase is possible. An EDX analysis showed that in addition to the expected element distribution of glass and silver residues of fluorine were present. We assume that the fluorine in the liquid phase was bound in the liquid and could not dissipate, as in the gas phase process.

Additionally, we evaporated the pure precursor in a heated vacuum cell and exposed a quartz plate with a 193 nm excimer laser at 18 ns pulse length and 0.057 mJ pulse energy, to investigate the possibility of SPA-based decomposition of the precursor from the gas phase. The structural deposition in the irradiated areas of the substrate shows that it is possible to decompose the precursor in a photolytic process by SPA. The deposited material consists of a fine granular structure and exhibits heights in the nm-range, depending on the applied pulse number. An EDX analysis was done after sputtering the substrate with a 30 nm gold layer.

The atomic element distribution is carbon (5.04 %), silicon (30.90 %), oxygen (62.31 %), gold (1.19 %) and silver (0.56 %). Due to the thin silver layers only a small amount of silver is obtained, but after subtraction of the quartz glass substrate background signal from the spectrum, it was obvious that the deposited layer consists almost of pure silver. No residues from the original precursor, like fluorine, were measured in the EDX spectrum.

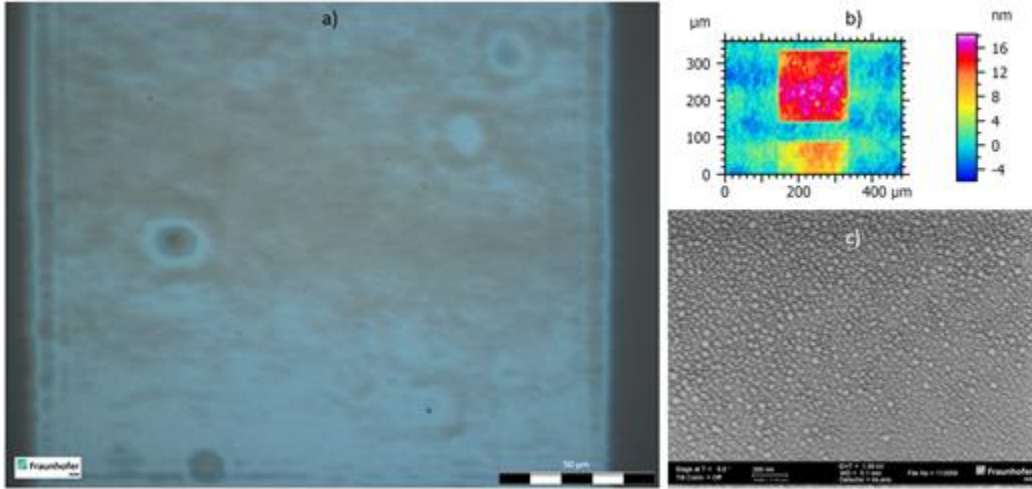


Fig. 2. Metallic depositions with a 193 nm excimer laser. (a) The square is deposited with an energy of 0.057 mJ and a pulse number of 1. (b) A square deposited with a pulse number of 800 is shown at the bottom and has a height of around 7 nm. The square deposited with a pulse number of 1000 is shown at the top and has a height of about 15 nm. (c) The granular structure of the deposited squares becomes evident in the SEM image.

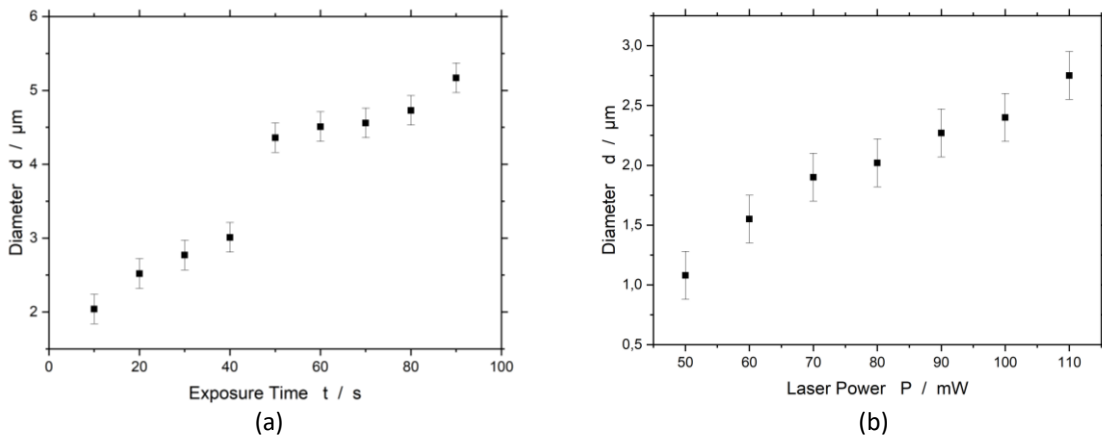


Fig. 3. Deposition of silver spots in pure, liquid precursor. (a) Diameter of the deposited spots as a function of the exposure time. The laser power was 117 mW. (b) Diameter of the deposited spots as a function of the laser power. The exposure time was 10 s.

Afterwards the possibility of decomposing the liquid precursor in a TPA process was demonstrated by using the Ti:Sapphire-laser, to determine the correlation between laser power, exposure time and deposited spot size. For that, the liquid precursor was placed in between two microscope cover glasses and was afterwards irradiated with fs-Laser of different exposure time and power. The deposited spot sizes show a linear correlation as a function of the exposure time and the laser power, respectively (Fig. 3). We assume that the step in the diameter's size between 40 s and 50 s (Fig. 3a) is an additional deposition effect, which we attribute to reflection of the laser beam at the already deposited metallic material and thereby a higher intensity in the focal region, leading to additional deposition of the precursor. A purely thermally induced deposition process could be ruled out experimentally by exposure of the substrate with a cw laser beam of 800 nm wavelength over one minute. No depositions could be detected in that case.

Based on the findings from the preliminary tests, the technique was transferred to the TPA-based deposition of metallic nanostructures from the gas phase. Firstly, experiments were made, to investigate the z-range in which a deposition on the substrate surface could be achieved.

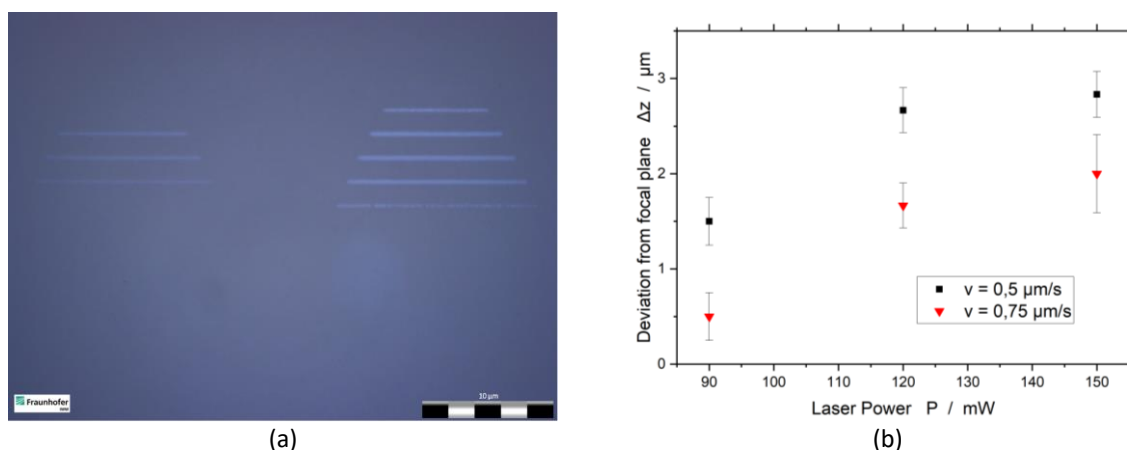


Fig. 4. (a) The lines at the right side were written with a scanning velocity of $0.5 \mu\text{m/s}$ and at the left side of $0.75 \mu\text{m/s}$. The lines from the same scanning velocity differ in their z-position from each other. With slower scanning velocity more lines are deposited and the deviation from the focal plane is enlarged. (b) The deviation from the focal pane as a function of scanning velocity and laser power.

In Fig. 4a, the deviation (Δz) from the focal plane (z_0) which is tolerable to get still deposition, is shown as a function of laser power and scanning velocity, respectively. Δz increases with growing laser power and decreases with increasing scanning velocity (Fig. 4b). All experiments were executed at a mean pressure of $1.53 \text{ mbar} \pm 0.50 \text{ mbar}$.

Vertically oriented lines were deposited with a laser power of 150 mW and diagonally deposited lines with a laser power of 75 mW (Fig. 5a). Both were written with the same scanning velocities from the top to the bottom, starting with $0.125 \mu\text{m/s}$ to $1.25 \mu\text{m/s}$. The lines deposited with 75 mW are always comparable with the lines deposited with 150 mW and doubled scanning velocity. This demonstrates that the relevant dose or energy input per unit length P/v is constant for successful deposition. For highest doses, the deposition on glass becomes above average (Fig. 5a, top). A possible explanation for that could be a reflection of light from the already deposited structures, increasing the intensity of light in the focal region, leading to a stronger decomposition of precursor molecules and, thereby to a disproportionate deposition rate. For very low doses (low laser power and/or high scanning velocities), no deposition is observable.

The corresponding line widths also increase with higher laser power and decrease with a higher scanning velocity (Fig. 5b). It is important to know exactly the relationship between these parameters to develop writing technologies and methods for manufacturing three-dimensional structures.

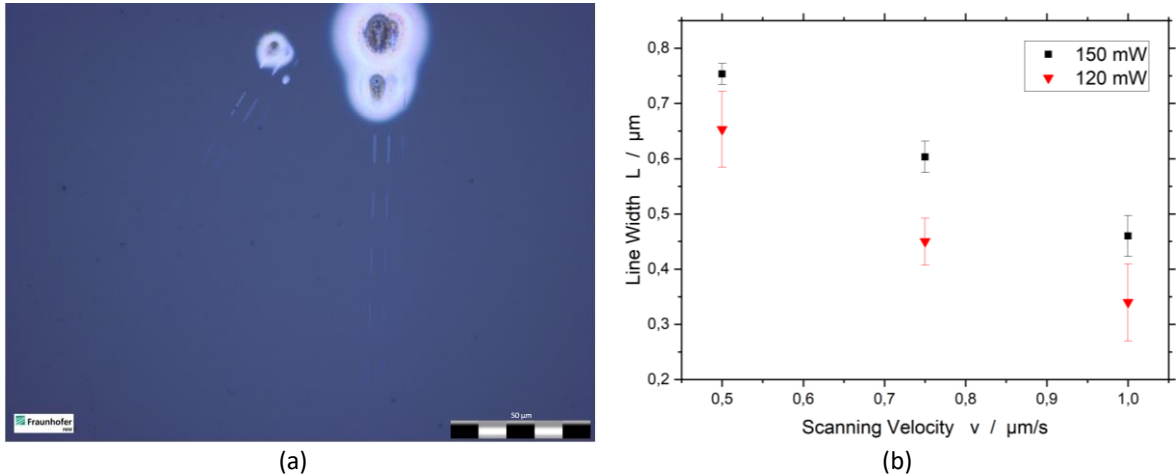


Fig. 5. (a) The vertical oriented lines were deposited with a laser power of 150 mW and the diagonal deposited with a laser power of 75 mW. The scanning velocity increases from top to bottom $v = [0.125, 0.25, 0.5, 0.75, 1.0, 1.25]$ $\mu\text{m/s}$. (b) Line width as a function of scanning velocity and laser power.

EDX measurements revealed that the deposited structures showed a high silver content, depending on the structure height. A single pass on the substrate with a scanning velocity of 0.5 $\mu\text{m/s}$ and a laser power of 120 mW deposits layers about 6 nm high. For these thin structures the substrate material was always evident in the EDX spectra. Stacking of several layers lead to thicker structures (>800 nm) that showed almost pure silver in the EDX spectra (Table 1).

Table 1. Element distribution of an EDX spectrum of an 800 nm thick structure (left) and a 450 nm thick structure on ITO (right).

Element	Weight%	Atomic%	Element	Weight%	Atomic%
C K	0.73	6.09	C K	0.88	5.32
Si K	0.62	2.20	Si K	2.52	6.54
Ag L	93.04	86.78	Ag L	68.76	46.43
In L	5.61	4.92	In L	20.13	12.77
O K	-	-	O K	5.90	26.88
Sn L	-	-	Sn L	1.43	0.88
Total	100		Total	100	

The SEM image in Figure 6a shows that the deposited lines have a smooth and compact morphology with low surface roughness. The lines were written at a speed of 0.5 $\mu\text{m/s}$ at a power of 120 mW and have a line width of 400 nm. The aspect ratio typically is in the range of 1:100. An example of a coherent two-dimensional structure is shown in Figure 6b. Here, the "Fraunhofer" lettering with a font size of 10 μm was deposited on a glass substrate at a scanning velocity of 1 $\mu\text{m/s}$ with a power of 150 mW.

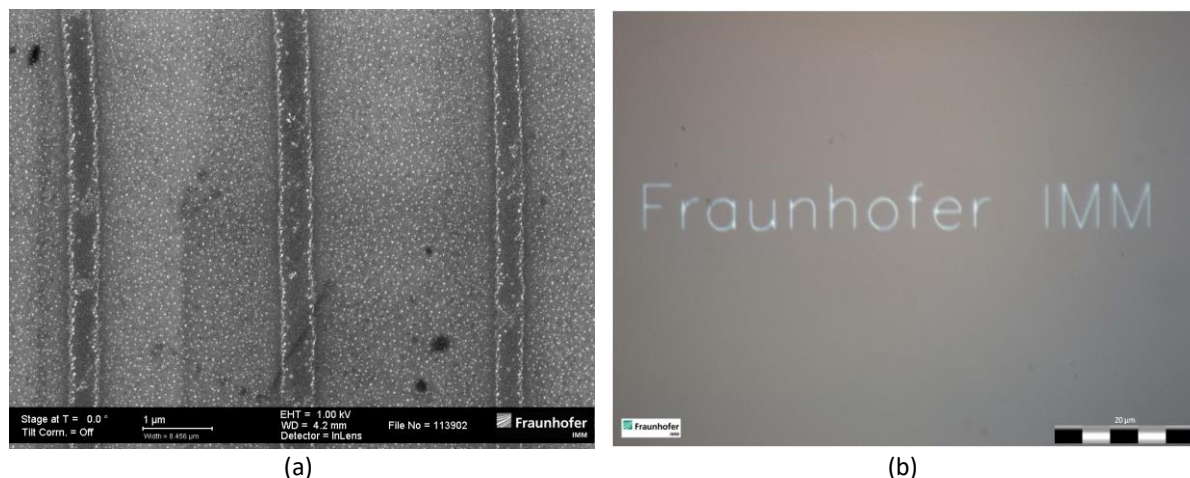


Fig. 6. (a) Thin Silver lines deposited on a substrate. In this case, in addition to the structures written by laser, a thin film, which is probably a residue of the gaseous precursor, had been deposited. (b) Fraunhofer lettering deposited with TPA from the gas phase.

4. Summary and outlook

We were able to demonstrate the deposition of two-dimensional silver nanostructures from the gas phase below the diffraction limit by means of two-photon-absorption. It could be shown that laser power and scanning velocity are essential influencing factors in the deposition process. We obtained high purity of silver structures, which was verified by EDX analysis. Clearly defined structures of size down to 400 nm could be deposited. The deviation from the focal plane at which deposition occurs could be determined and will be taken into account for further writing methodologies, especially when extending the method to the third dimension. The concentration of the organometallic precursor in the gas phase also plays an important role in the deposition process and needs further investigation to maximize the reproducibility of the process. The results of these investigations will be presented elsewhere. First quasi-three-dimensional structures could be built up in preliminary tests. In further experiments, parameters are to be optimized to manufacture free-standing three-dimensional structures in the nanometer range. These structures could be used for the construction of meta-surfaces and enable optical sensors with the help of plasmonic effects. Further organometallic precursors are to be examined for photolytic decomposition and used in direct laser writing of metallic structures from the gas phase.

Acknowledgements

We thank the German ministry of education and research BMBF for supporting the project LAMETA under grant number 13N14948.

References

- A. Ishikawa et al., Two-Photon Fabrication of Three-Dimensional Metallic Nanostructures for Plasmonic Metamaterials, *J. Las. Mic. Nan. Eng.* 7 (2012) 1
- A. Radke et al., Fabrication of dielectric and metallo-dielectric 3D nanostructures by direct laser writing and electroless plating, *Proc. of SPIE Vol. 7585 75850M-1*
- A. Radke et al., Three-Dimensional Bichiral Plasmonic Crystals Fabricated by Direct Laser Writing and Electroless Silver Plating, *Adv. Mat.* Vol. 23 (2011) 27, pp. 3018–3021
- Barth, S., Huth, M., Jungwirth, F., 2020. Precursors for direct-write nanofabrication with electrons, *J. Mater. Chem. C*, 8, 15884
- Hirt, L., Reiser, A., Spolenak, R., Zambelli, T., 2017. Additive Manufacturing of Metal Structures at the Micrometer Scale, *Adv. Mater.*, 29, 1604211
- Lehmann, O., Stuke, M., 1991. Generation of three-dimensional free-standing metal micro-objects by laser chemical processing, *Appl. Phys. A* 53, p. 343-345
- Seniutinas, G., Gervinskas, G., Verma, R., Gupta, B. D., Lapierre, F., Stoddart, P. R., Clark, F., McArthur, S. L., Juodkazis, S., 2015. Versatile SERS sensing based on black silicon, *Opt. Express* 23, p. 6763-6772 (2015)
- Wong, Z., Wang, Y., O'Brien, K., Rho, J., Yin, X., Zhang, S., Fang, N., Yen, T.-J., Zhang, X., 2017. Optical and acoustic metamaterials: Superlens, negative refractive index and invisibility cloak, *Journal of Optics*. 19.
- Xu, B.-B., Xia, H., Niu, L.-G., Zhang, Y.-L., Sun, K., Chen, Q.-D., Xu, Y., Lv, Z.-Q., Li, Z.-H., Misawa, H. and Sun, H.-B., 2010. Flexible Nanowiring of Metal on Nonplanar Substrates by Femtosecond-Laser-Induced Electroless Plating, *Small*, 6: p. 1762-1766.
- Yokota, Y., Ueno, K., Juodkazis, S., Mizeikis, V., Murazawa, N., Misawa, H., Kasa, H., Kintaka, K., & Nishii, J., 2009. Nano-textured metallic surfaces for optical sensing and detection applications, *Journal of Photochemistry and Photobiology A: Chemistry*, 207(1), p. 126-134.
- Zarzar, L. D., Swartzentruber, B.S., Harper, J. C., Dunphy, D. R., Brinker, J., Aizenberg, J., Kaehr, B., 2012. Multiphoton Lithography of Nanocrystalline Platinum and Palladium for Site-Specific Catalysis in 3D Microenvironments, *Journal of American Chemical Society* 134 (9), p. 4007-4010